

PHASE EQUILIBRIA IN THE THORIUM-TANTALUM SYSTEM

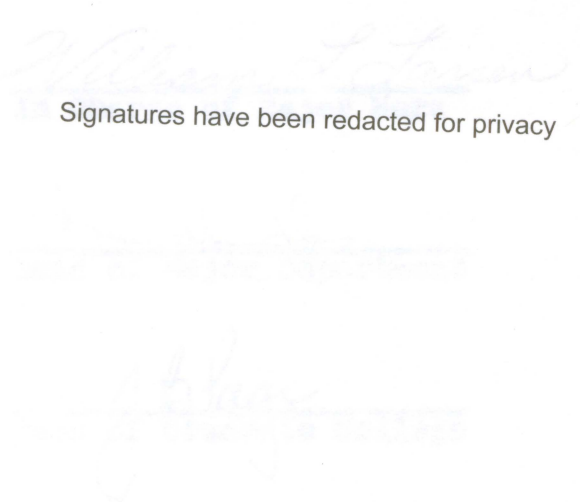
by

Omar Dale McMasters

A Thesis Submitted to the
Graduate Faculty in Partial Fulfillment of
The Requirements for the Degree of
MASTER OF SCIENCE

Major Subject: Nuclear Engineering

Approved:



Signatures have been redacted for privacy

Iowa State University
Of Science and Technology
Ames, Iowa

1961

TABLE OF CONTENTS

	Page
ABSTRACT	1
INTRODUCTION	2
APPARATUS AND PROCEDURES	5
EXPERIMENTAL RESULTS	19
SUMMARY	47
ACKNOWLEDGMENTS	48
REFERENCES CITED	49
APPENDIX	51

ABSTRACT

X-ray, electrical resistance, thermal and metallographic methods were used to determine the phase diagram of the thorium-tantalum system. The diagram is of the simple eutectic type with a eutectoid reaction associated with the thorium α - β transformation. The solubility of tantalum in thorium is approximately 0.4 weight per cent at the eutectic temperature and approximately 0.2 weight per cent at the eutectoid temperature of 1338°C. The room temperature solubilities are nil and the solubility of thorium in tantalum is approximately 0.2 weight per cent at the eutectic temperature of 1565°C.

INTRODUCTION

Phase diagrams constitute the major source of information which contributes to a better understanding of the behavior of metals and alloys. Emphasis has recently been placed upon basic research as the slower, but more certain, means to the solutions of the materials problems associated with the production of economically competitive nuclear power. This investigation was undertaken in order to establish the constitutional diagram of the thorium-tantalum alloys and to increase the knowledge of thorium and tantalum metallurgy.

Thorium, a fertile, nonfissionable material is a potential solution to some of the problems associated with power reactor economics. Power production by nuclear fission coupled with a positive net fuel supply could be realized by the inclusion of thorium as a blanket material in a reactor design. From the nuclear standpoint, the use of thorium is particularly appealing since the fissionable uranium-233 conversion product is superior to and less hazardous to handle than plutonium. Pure thorium is quite soft and ductile. It tends to tarnish in air at room temperature, especially if the surface is disturbed. Chiotti (3) has reported that thorium has a face centered cubic structure at temperatures up to $1360 \pm 10^\circ\text{C}$. The lattice spacing for the room temperature form is 5.0843 \AA according to Evans and Raynor (5). The body centered cubic form exists from 1360°C to the $1750 \pm 10^\circ\text{C}$ melting point (3).

The properties of this highly reactive material vary with the purity and most of the information in the literature pertains to the effects of contamination on the properties of thorium. Property values obtained from studies of this nature are generally obtained by extrapolating the data to zero impurity content.

The relatively high neutron absorption cross section of tantalum depicts it as an unfavorable reactor material. However, because of its high temperature mechanical properties and its resistance to erosion and corrosion, tantalum is competitive with such materials as niobium, steels and ceramics in the nuclear energy program. Pure tantalum is a soft and very ductile metal. Williams and Pechin (13) reported a melting point of 2940°C for the tantalum used in this investigation and it exists in the body centered cubic form up to this temperature. Being a less common and expensive metal, the metallurgical potentialities of tantalum have not been explored to as great an extent as have some of the more abundant materials. Consequently, tantalum metallurgy and technology are in their early developmental stages.

The thorium-tantalum phase diagram and the observations made during alloy and specimen preparations of this investigation contribute to the information needed in the development of thorium-tantalum alloys for specific uses.

A forecast of the expected behavior of tantalum upon alloying it with thorium and other elements is presented by Miller (8). The forecast is based on the collective results from the considerations of Hume-Rothery's rules, modified Hildebrand's 'solubility parameters' (as discussed by Mott) and Pauling's 'electronegativities' (according to Haissinsky). The results predicted that thorium is a marginal case for liquid immiscibility with tantalum. Also, the size factor of thorium is unfavorable for solid solution formation and compounds are unlikely to form with tantalum. That the thorium-tantalum alloy system is most probably of the eutectic type was deduced from the diagrams of the thorium-group V-B alloy systems as compiled by Rough and Bauer (10).

APPARATUS AND PROCEDURES

Most of the apparatus used to obtain the data in this investigation has become standard equipment in metallurgical research laboratories. Detailed descriptions of the basic equipment are available in the references cited. Special equipment and procedures needed because of the high temperatures at which most of the data were obtained are described below. The majority of the work at elevated temperatures was performed under a pressure of 10^{-6} mm Hg or less. The exceptions are arc-melting and some quenching of specimens, both of which involved the filling of evacuated chambers with an inert gas.

Preparation of Alloys

Component metals

The tantalum used in the preparation of the alloys was supplied by the Fansteel Metallurgical Corporation and was specified as high purity sheet. The impurity content of this metal and that of thorium is given in Table 1. The crystal-bar thorium used in this investigation was prepared by the author in the Ames Laboratory. The iodide process as described by Veigel, Sherwood and Campbell (11) was duplicated on a 200-300 gram batch basis and the thorium is of high purity.

Table 1. Analysis of the component metals*

Impurity	Content in tantalum (ppm)	Content in thorium (ppm)
Carbon	16 ^a	75 - 100 ^a
Oxygen	50 ^b	50 - 150 ^b
Nitrogen	22 ^b	75 - 150 ^a
Hydrogen	1 ^b	4 ^b
Iron	40 ^a	20
Titanium	20	
Manganese		20
Aluminum		30
Beryllium		20
Calcium		20
Magnesium	Faint trace	20
Silicon	20	50
Zirconium		200
Nickel		20
Niobium	Faint trace	

*Spectrographic analysis unless otherwise noted.

^aChemical analysis.

^bVacuum fusion analysis.

Melting and homogenizing

A tungsten-electrode arc-furnace was used to melt the alloys. The depressions in the water-cooled copper hearth provide a means of obtaining two sizes of button-shaped ingots as well as rod-shaped samples. Melting of the alloys under a helium atmosphere was preceded by melting "getter" charges of both zirconium and thorium in order to reduce the impurity content of the helium. Charges of intended compositions were melted several times and were turned over between melts in an attempt to make them homogeneous. Losses of no more than 0.05 gm of the 60 to 80 gm charges during the melting procedure were neglected and the data from this investigation are based on the intended composition. The large difference between the melting points of the component metals made melting and homogenizing of the alloys difficult. Splattering of the molten charge was usual and necessitated power reductions in the arc in order to avoid sample losses and to facilitate ingot shaping. The resulting ingots were not homogeneous since the lower melting eutectic constituent tended to form a shell around the higher melting center portion which was dendritic in nature. This layering effect can be explained on the basis of the cooling process of the molten charge and represents the first indication that a region of liquid immiscibility might exist in the thorium-tantalum system. Cold-working and heat treatments usually

preceded the taking of data in order to increase the homogeneity of the specimens. Special methods of specimen preparations and heat treatments are described in the sections dealing with the individual analyses of this investigation.

Fabrication

Melting point bars were prepared by milling smooth the surfaces of slabs cut from the arc-cast buttons and then milling the center portion until a necked-down specimen was formed, as shown by Rogers and Atkins (9). No difficulties were encountered in the sectioning and milling operations. Cold-reductions of 60 per cent of the thickness were made on portions of the employed melting point bars by the use of a rolling mill. Heat treatments at various temperatures followed the cold working of these specimens and microscopic examination of the resulting structures completed the experiment. Cold working of this nature produced cracks in the samples in which dendritic segregation was prevalent.

Resistance-temperature and X-ray diffraction specimens were prepared by swaging the arc-cast rods into wires. All compositions of the thorium-tantalum samples could be swaged from 0.250 inch diameter rods to 0.030 inch diameter wires without intermediate heat treatments. Some flaking of the dendritic phase was noted in the swaging of samples in the intermediate composition range. This flaking action was eliminated in the preparation of 10 mil diameter X-ray

diffraction specimens by choosing samples in the 1.0 to 10 weight per cent Ta-Th and 90 to 99 weight per cent Ta-Th composition ranges.

Melting Point Determinations

The apparatus used to obtain melting point data has been described by Williams (14). Two large copper clamps attached to two water-cooled electrodes serve to hold a specimen which is heated by its own resistance. A variable transformer provides the current for controlled heating of the specimen. The melting point bars were machined from sections cut from the as-cast ingots. Temperatures were measured by a Leeds and Northrup disappearing filament type optical pyrometer. A small hole with a depth to diameter ratio of about 5 to 1 drilled in the center of the necked-down portion of the bar served as a miniature black body. Both the surface or apparent temperature and the hole or black-body temperature readings were recorded. An extrapolation of the black-body versus surface temperature data allowed the liquidus temperatures to be approximated. The extrapolation process requires the assumption that the emissivity of the surface as a function of temperature is the same both below and above the solidus temperature. Depth to diameter ratios of four or less did not give adequate black-body conditions in that the sides and bottom of the hole were visible at high temperatures. Ratios of six or more required the formation of considerable

amounts of liquid before the black-body conditions were disrupted by filling of the hole; thus, solidus values obtained from experiments in which the specimens had holes with ratios greater than five were usually too high. Intermediate heat treatments of one to two hours at 1300°C and 1400°C tended to improve the homogeneity of the specimens.

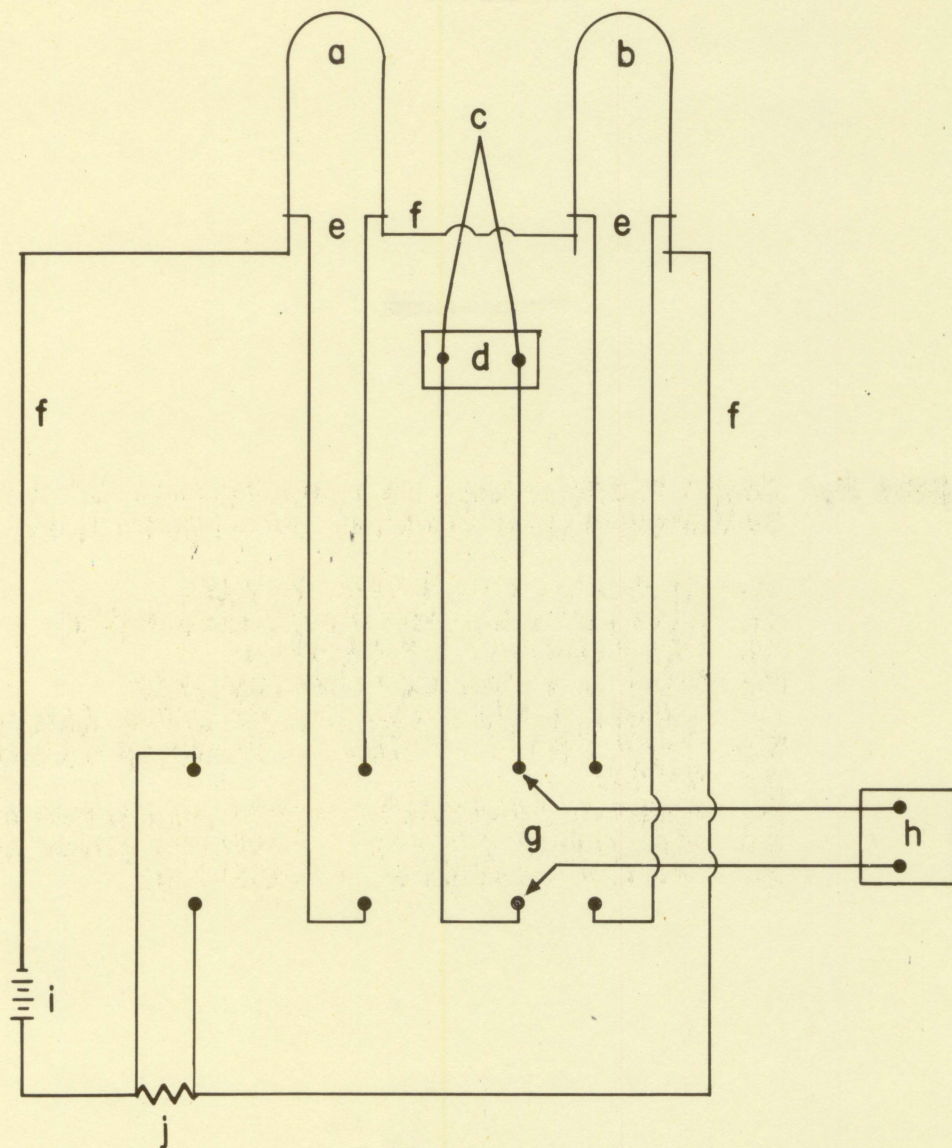
Electrical Resistance versus Temperature

Electrical resistivity is a property that varies markedly with temperature change. This property was used to locate the alpha to beta transformation isotherm for alloyed and unalloyed thorium. Electrical resistance data, rather than specific resistivity data, were obtained because they clearly showed transformation points without requiring the determination of precise specimen dimensions. The basic circuit used to obtain the data which was needed to calculate the electrical resistance of the specimens at various temperatures is shown in Figure 1.

Preliminary data were obtained from experiments in which wire specimens were heated by their own resistance. The power supply for heating the specimens consisted of nine 6-volt batteries connected in series. The specimens were clamped between two water-cooled copper electrodes in an evacuated chamber. An optical pyrometer was used to measure the surface temperature of the specimens. The surface to black-body temperature relationship obtained during the

Figure 1. Basic circuit used in measurements of electrical resistance as a function of temperature.

- a. Specimen, unalloyed thorium
- b. Specimen, alloyed thorium-tantalum
- c. Thermocouple, Pt-Pt+13%Rh
- d. Cold junction for thermocouple
- e. e.m.f. leads (0.01 in. diameter tantalum wire)
- f. Power leads (0.01 in. diameter tantalum wire)
- g. Switch
- h. Rubicon potentiometer and galvanometer
- i. Two 6-volt storage batteries, power supply
- j. Standard 0.1000 ohm resistance



melting point determinations was used to approximate the actual temperature of the specimens. The surface to black-body relationship is based on temperatures obtained from flat surfaces while the temperatures in these experiments were measured on curved surfaces of wire specimens. No correction factor for this difference in the temperature measurement conditions was applied to the data, so the actual specimen temperature values are at most approximations. The voltage drops across the specimens and the standard resistance were measured potentiometrically and the resistance of the specimen was calculated by the method described by Rogers and Atkins (9). In this arrangement the power supply used to heat the specimens was included in the e.s.f. measuring circuit and caused the potentiometric measurements to be somewhat inconsistent.

In another arrangement two specimens, usually one thorium and a thorium-tantalum alloy, were connected in series with a standard resistor. Ten mil diameter tantalum potential leads were spot welded, under a helium atmosphere, to the specimens. A 6-volt storage battery completed the circuit and eliminated the troubles due to the power supply in the arrangement described above. The specimens were heated under vacuum by a silicon-carbide resistance heating element furnace. The voltage drops across the specimens and the standard resistance were measured potentiometrically. The temperature was

measured by a Pt-Pt-13Rh thermocouple and resistance-temperature data over a 30°C to 1425°C range were obtained from this arrangement.

X-ray Diffraction Methods

X-ray diffraction patterns were obtained from specimens of various forms. Both nickel-filtered copper radiation and zirconium-filtered molybdenum radiation were used in conjunction with a General Electric (Model XRD-4) X-ray unit. A standard Debye-Scherrer type camera, a self-focusing back-reflection camera and a Norelco diffractometer were used to obtain the X-ray data.

Powders were filed from the melting point specimens and heat treated at 650°C for 36 hours in order to relieve the strains due to the filing process. An exposure of 6 to 8 hours in a Debye-Scherrer type camera usually yielded a satisfactory pattern. Room temperature solubility limits were determined from the resulting lattice parameter data by the method described later.

Thin sheet specimens were prepared by rolling and taped to the perimeter of the back-reflection camera. Prior to camera mounting, these specimens were heat treated at high temperatures for several hours in order to relieve the strains due to the cold working. The specimens were quenched by simultaneously flooding the evacuated heating chamber with helium and cutting the power used to heat the specimens.

The more significant X-ray data of this investigation were obtained from quenched wire specimens using a standard Debye-Scherrer camera and 6 to 8 hour exposures to copper K alpha radiation. Since the procedures for preparing a specimen are of importance in obtaining accurate lattice parameters, they are presented here in detail. Samples of various compositions were swaged to 0.080 inch diameter rods. The rod sample was cleaned and inserted into a 60% Cu-Ni tube (0.125 inch O.D. and 0.085 inch I.D.). The jacketed sample was swaged to 0.080 inch in diameter. The jacketing and swaging steps were repeated until a total of four Cu-Ni jackets covered the sample. Swaging was continued through the 0.031 inch die and the jackets were removed by dissolution in a nitric acid solution. The resulting wire sample was 0.010 inch in diameter and was fairly uniform in cross section. In order to avoid air contamination, the samples were stored under carbon tetrachloride. A three to four inch long specimen was cut from the wire and placed between two water-cooled copper electrodes for heat treatment. Contamination of the specimen during the heat treatment was held to a minimum since very little degassing of the evacuated heating chamber occurred and helium was not used as a quenching agent. The specimen was heated by its own resistance and the massive cooled copper electrodes provided a fairly effective quench by thermal conduction when the power used to heat the

specimen was turned off. Correction factors for the sight glass and the non-black-body conditions were applied to the surface temperature readings which were measured by means of an optical pyrometer.

The diffractometer equipment was used for phase identification of some metallographic specimens using standard procedures.

Metallography

The metallographic analysis of this alloy system involved the use of a Vickers projection microscope and standard polishing equipment. The polishing and etching procedures were complicated by the nature of the alloys. The eutectic constituent is considerably softer and less resistant to attack by etchants than is the dendritic phase. Consequently, the eutectic phase was usually scratched and pitted during these procedures. The more durable (generally dendritic) phase was left in relief making it difficult to resolve the details of the microstructures. For the tantalum rich alloys, the best results were obtained by the following procedure. Coarse polishing was done on non-lubricated silicon carbide papers followed by polishing on a water lubricated canvas covered wheel charged with 400 grit silicon carbide powder. Final polishing was done on Ab Microcloth covered wheels charged with diamond compounds using alcohol as a lubricant. A chemical etchant consisting of a solution of equal parts of

concentrated H_2SO_4 and HNO_3 and 48% HF was applied by immersing the sample for 30 to 60 seconds.

The thorium-rich and eutectic-rich samples required special attention during the polishing procedure. After the coarse polishing, as described above, was completed, the alloys were polished on AB Microcloth covered wheels using a water lubricant and 15 micron Al_2O_3 and Linde A abrasives. A fairly effective electropolishing technique completed the polishing procedure and also served as an etchant. The most suitable electrolyte was found to be a solution of 2 gm $(CH_3)_4NOI$ in 50 ml acetic acid and 5 ml glycerine. Polishing for 30 seconds at 20 volts and 0.2 amperes yielded relatively scratch-free surfaces.

A cathodic etching apparatus described by Carlson, Williams, Rogers and Manthos (2) was used to reveal the structures of some of the specimens for microscopic examination.

A chemical etchant used throughout the metallographic study consisted of a solution of one part concentrated HNO_3 and four parts H_2O . About 0.1 gm of Na_2FSiO_4 was added to about 200 ml of this solution and the etchant was applied by swabbing the specimens for about one minute.

Miscellaneous Equipment

Several standard furnaces were used to heat treat the samples at various stages of the investigation. A tantalum

tube resistance furnace mounted vertically between two water-cooled copper electrodes proved to be most versatile in the 1400°C to 2000°C temperature range. Induction heating was utilized in some of the heat treating operations.

EXPERIMENTAL RESULTS

The constitutional diagram shown in Figure 2 is based on the results obtained from melting point determinations, X-ray diffraction data, resistance-temperature plots and metallographic observations. Figure 3 is a plot of most of the data from which the thorium-tantalum diagram was drawn.

Solidus and Liquidus Data

Melting point determinations were used to obtain the data which established the temperature of the eutectic reaction isotherm and approximated the position of the liquidus lines. The data obtained from the necked-down bar specimens have been plotted in Figure 3 and are listed in Table 2. The $1565 \pm 10^\circ\text{C}$ eutectic temperature was determined by observing the temperature at which the molten metal disrupted the black-body conditions of the hole by causing a dark spot to appear at the bottom of the hole. An accuracy of $\pm 10^\circ\text{C}$ is claimed, since the 1565°C value has been consistently reproduced and the precision of the pyrometric measurements is about $\pm 5^\circ\text{C}$ at this temperature. In a few instances the melt only created a shadow within the hole and a dark spot would not appear until more melt was forced at slightly higher temperatures. All temperatures obtained by the use of an optical pyrometer were corrected for the effect of the cover glass. The eutectic temperature was confirmed by the results obtained

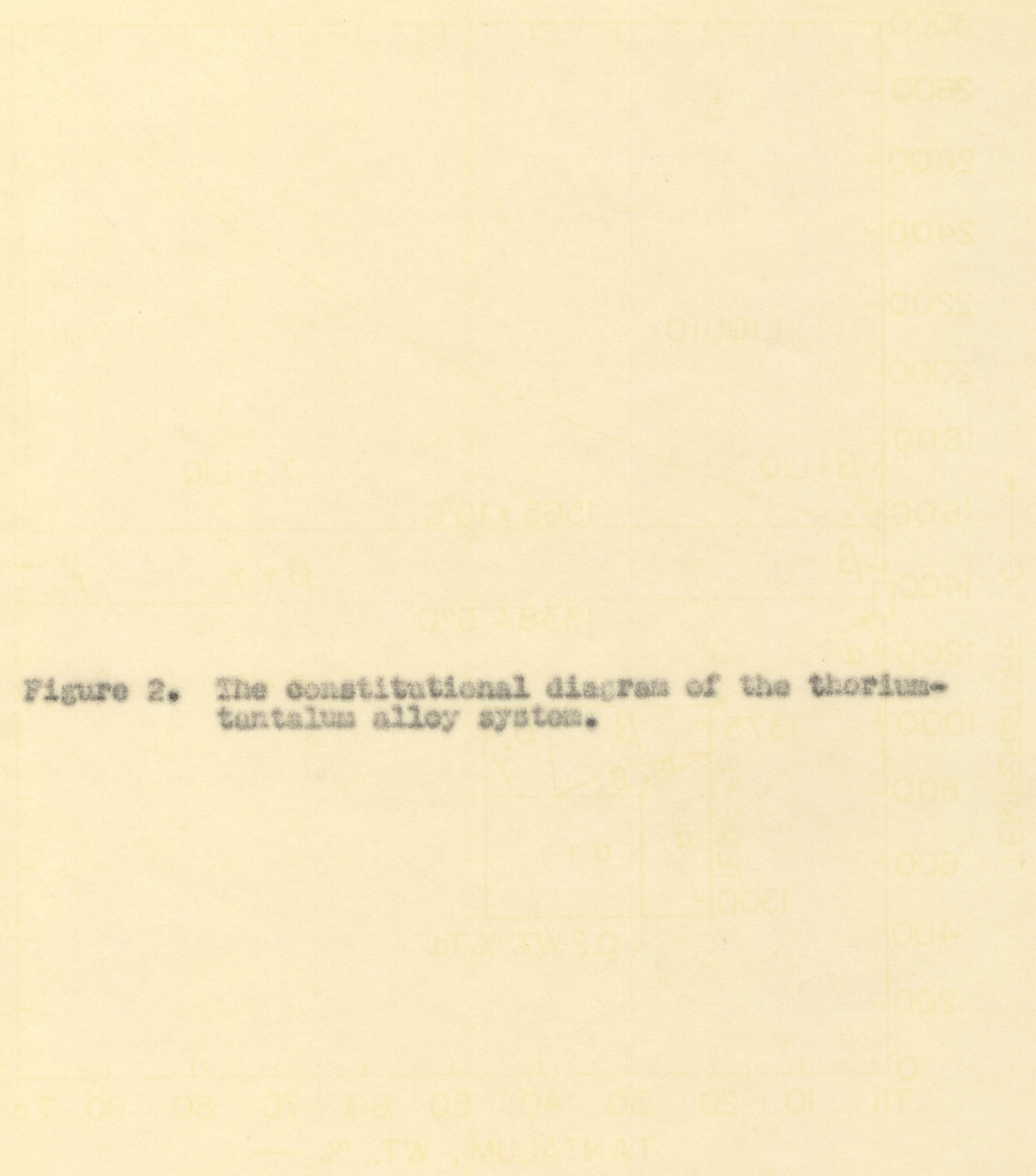
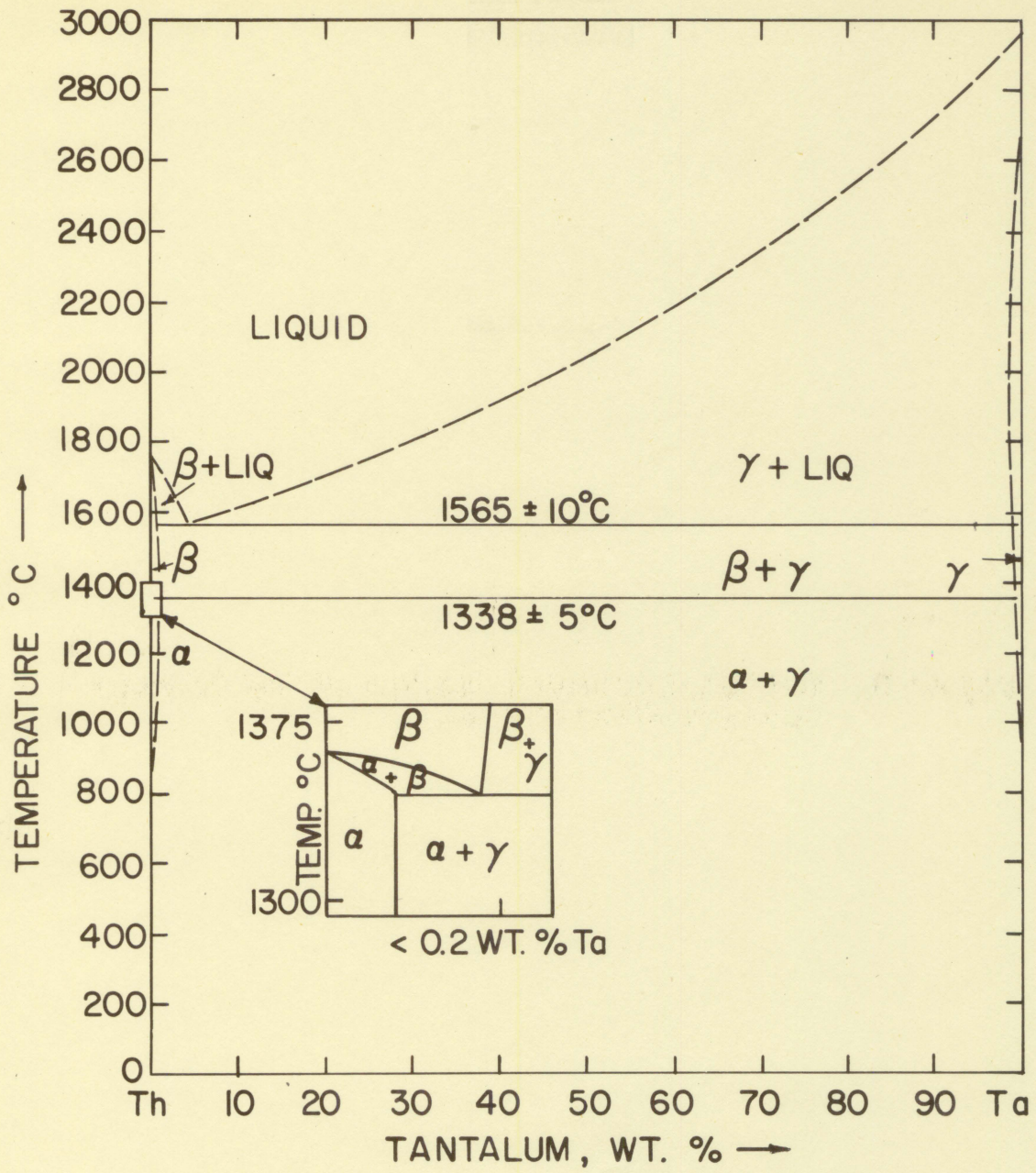


Figure 2. The constitutional diagram of the thorium-tantalum alloy system.



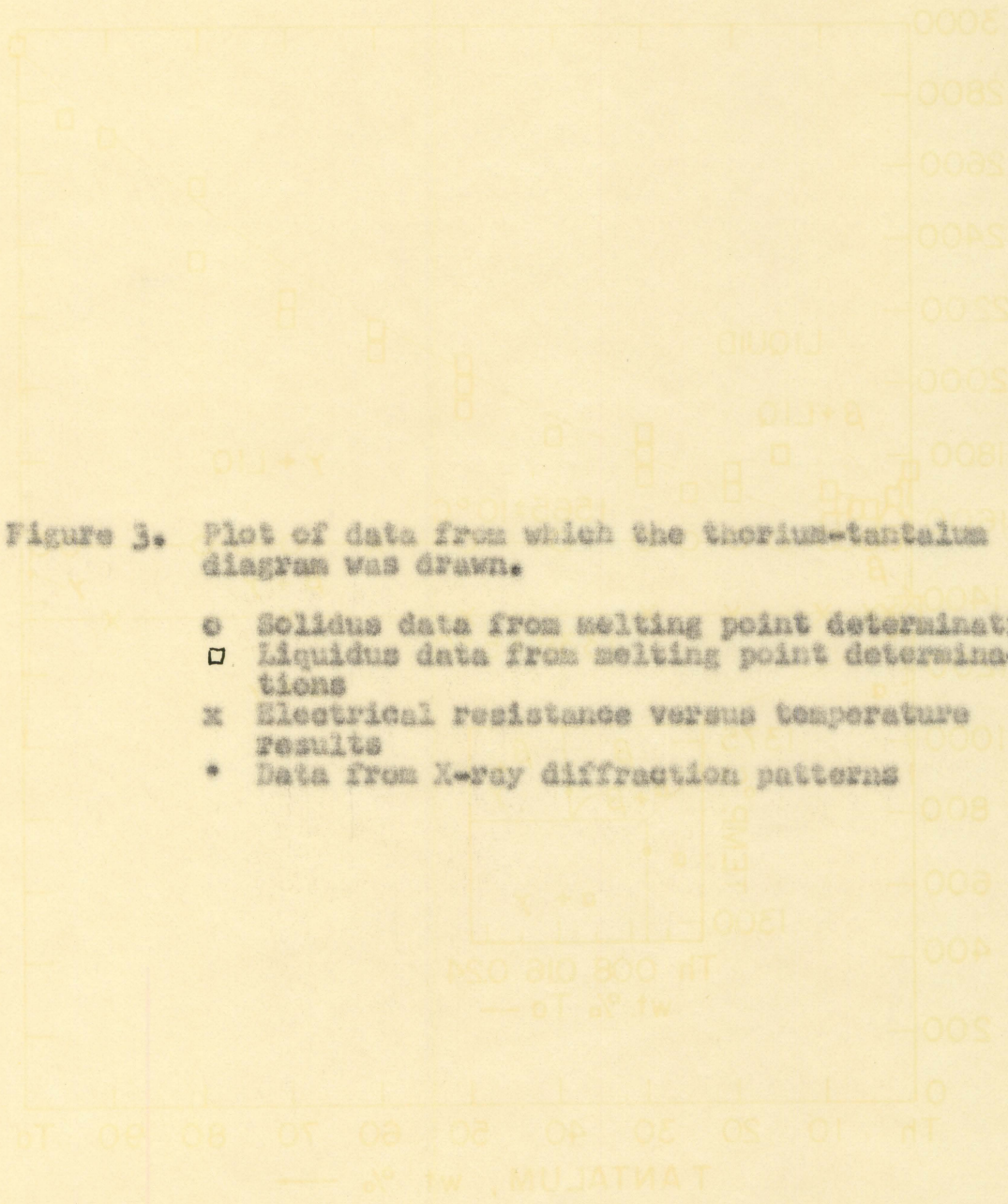


Figure 3. Plot of data from which the thorium-tantalum diagram was drawn.

- o Solidus data from melting point determinations
- Liquidus data from melting point determinations
- x Electrical resistance versus temperature results
- Data from X-ray diffraction patterns

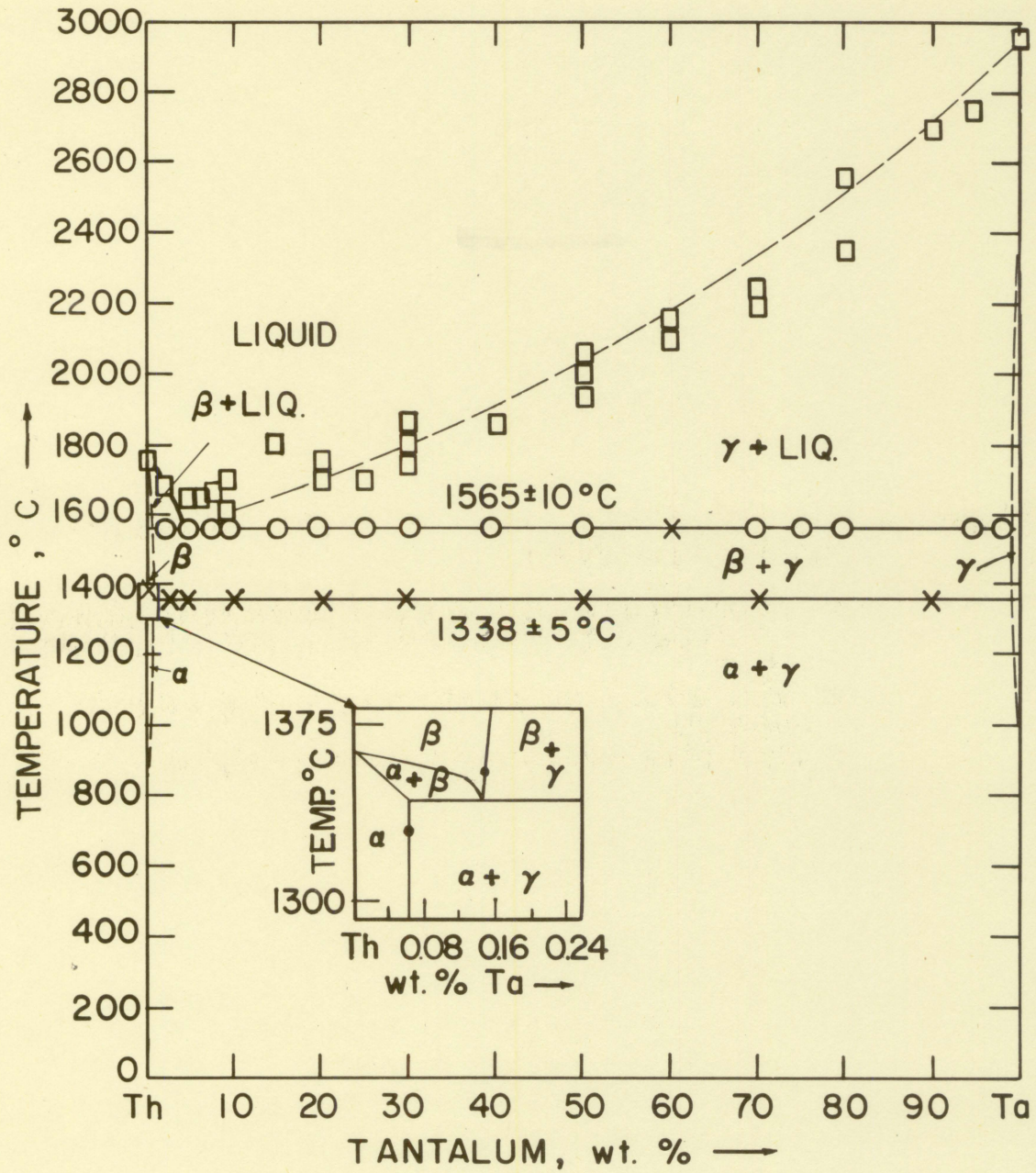


Table 2. Data from the melting point determinations

Wt. % Ta-Th	Solidus, °C	Liquidus, °C
thorium	melting points of 1700°C and 1725°C	
3.1	1563 ^a	1685
5.0	1565 ^a	1640
6.0	1565	1650
7.5	1563 ^a	1620
9.0	1563	1680
10.6	-----	1700
15.0	1565	1800
20.0	1565 ^a	1725
25.0	1570 ^b	1700
30.0	1566 ^b	1800
40.0	1565	1850
50.0	1566 ^b	1975
60.0	-----	2125
70.0	1573	2230
75.0	1568	2025
80.0	1568 ^a	2475
90.0	1570	-----
95.0	1570	2750
98.0	1575	-----
tantalum	melting point 2940°C ^c	

^aAverage of two measurements.

^bAverage of three measurements.

^cReported by Williams and Fochin (13).

from high temperature resistance experiments. A sharp rise in the resistance was noted in the resistance curves at $1565 \pm 10^\circ\text{C}$. An optical pyrometer sighted on the surface of 0.05 inch to 0.07 inch diameter wire specimen was used to measure the temperature. Both a sight glass correction factor and a surface temperature to black-body temperature correction factor, which was obtained during the melting point experiments, were applied to the temperature readings.

The liquidus lines were located by observing the temperature at which the specimen melted in two. The liquidus points determined in this manner are low, since the tantalum rich specimens invariably broke in two before completely melting and the eutectic rich specimens had a tendency to form hot spots due to the formation of liquid. Furthermore, the extrapolations of the black-body versus surface temperature relationships are known to be in error for the higher liquidus temperatures, since the emissivity of the surface varies when liquid is present. The liquidus lines appear as dashed lines in the diagram, since a $\pm 50^\circ\text{C}$ accuracy limit of the data usually resulted.

Experiments designed to improve the accuracy of the liquidus points met with a great deal of difficulty. In these experiments a tantalum tube resistance heater mounted vertically between two water cooled copper electrodes was used to heat powder compacts of various compositions. One

hour heat treatments at 50°C intervals over the 1550°C to 1750°C temperature range were completed on compacts of compositions 10, 20 and 40 weight per cent Ta-Th. The specimens were removed after each heat treatment and observed microscopically. The object of the experiment was to detect the temperature at which the tantalum particles were changed from rounded globules to fine dendrites, which would form when the melt solidified during the quenching process that followed each heat treatment. The absence of tantalum globules would indicate that the specimen had been above the liquidus temperature of the alloy in question. Sight glass fogging during the outgassing and heat treating stages caused temperature measurements by optical means to be in error and slowed down the experimental procedures. The use of BeO crucibles as containers introduced impurities in the specimens in the form of thorium oxides, some of which were present in the original compacts. The use of tantalum crucibles as containers caused variations in the intended compositions of the specimens due to reaction of the melt with the walls of the container. Failures in the vacuum equipment and resistance heaters provoked the discontinuance of these experiments. The liquidus data that resulted from both of these methods are included in Figure 3 and Table 2.

The eutectic composition was tentatively placed at 7 weight per cent Ta-Th by extrapolating the liquidus lines

that resulted from the melting point experiments to the solidus temperature. Metallographic evidence, which is more reliable and which is presented in a later section, established the eutectic composition at 4 weight per cent Ta-Th.

Effects of Tantalum on the Transformation of Thorium

The data obtained by resistance-temperature methods were used in conjunction with X-ray diffraction results in order to determine the nature of the solid state reaction which is associated with the allotropic transformation of thorium. This portion of the diagram is shown in the insert in Figures 2 and 3.

The resistance-temperature data obtained from the arrangement which used a d.c. power supply to heat a wire specimen by its own resistance and which relied upon optical pyrometer temperature measurements indicated that the transformation temperature of thorium is lowered upon the addition of tantalum. From this arrangement the average temperature of the transformation of thorium in the alloyed specimens was found to be $1361 \pm 15^\circ\text{C}$ and that for the unalloyed thorium specimens was $1381 \pm 15^\circ\text{C}$. The $\pm 15^\circ\text{C}$ and accuracy limits of these values as compared to the 20°C temperature difference obtained in the analysis demanded the use of an arrangement from which more accurate data could be obtained. The mention of a few of the factors that contributed to the

$\pm 15^{\circ}\text{C}$ accuracy limits and their approximate effects on the data will help to explain the reasons for seeking a different arrangement. The temperature measurements were made with an optical pyrometer and the not-too-well established black-body to surface temperature correction factors were applied to the readings. A relatively large increase in the resistance of the specimens at the transformation temperature tended to heat the specimen and the most critical data therefore had to be eliminated. The non-uniform heating along the wire (cooler near the ends) created a wide range of temperatures over which the transformation took place. Although the accuracy range of the values obtained by this method is wide, the results indicated that the addition of tantalum to thorium lowers the transformation temperature and from this it can be concluded that a eutectoidal arrangement probably develops as a result of the alpha to beta transformation in thorium.

The apparatus and procedures were altered in order to eliminate most of the shortcomings of the above method. The potential drops across two specimens (one alloyed and one thorium) were measured potentiometrically at various temperatures. The resistances of the specimens were calculated on the basis of the e.m.f. information from the specimens and a standard resistance which is shown in the circuit in Figure 1. A Pt-Pt+13%Rh thermocouple was used to measure the temperatures and the thermocouples were calibrated against

a new thermocouple after each run. Temperature readings with an accuracy of $\pm 2^\circ\text{C}$ were obtained from this arrangement. Table 3 lists the results obtained from several experiments, and Figure 4 is a plot of the data from a typical experiment.

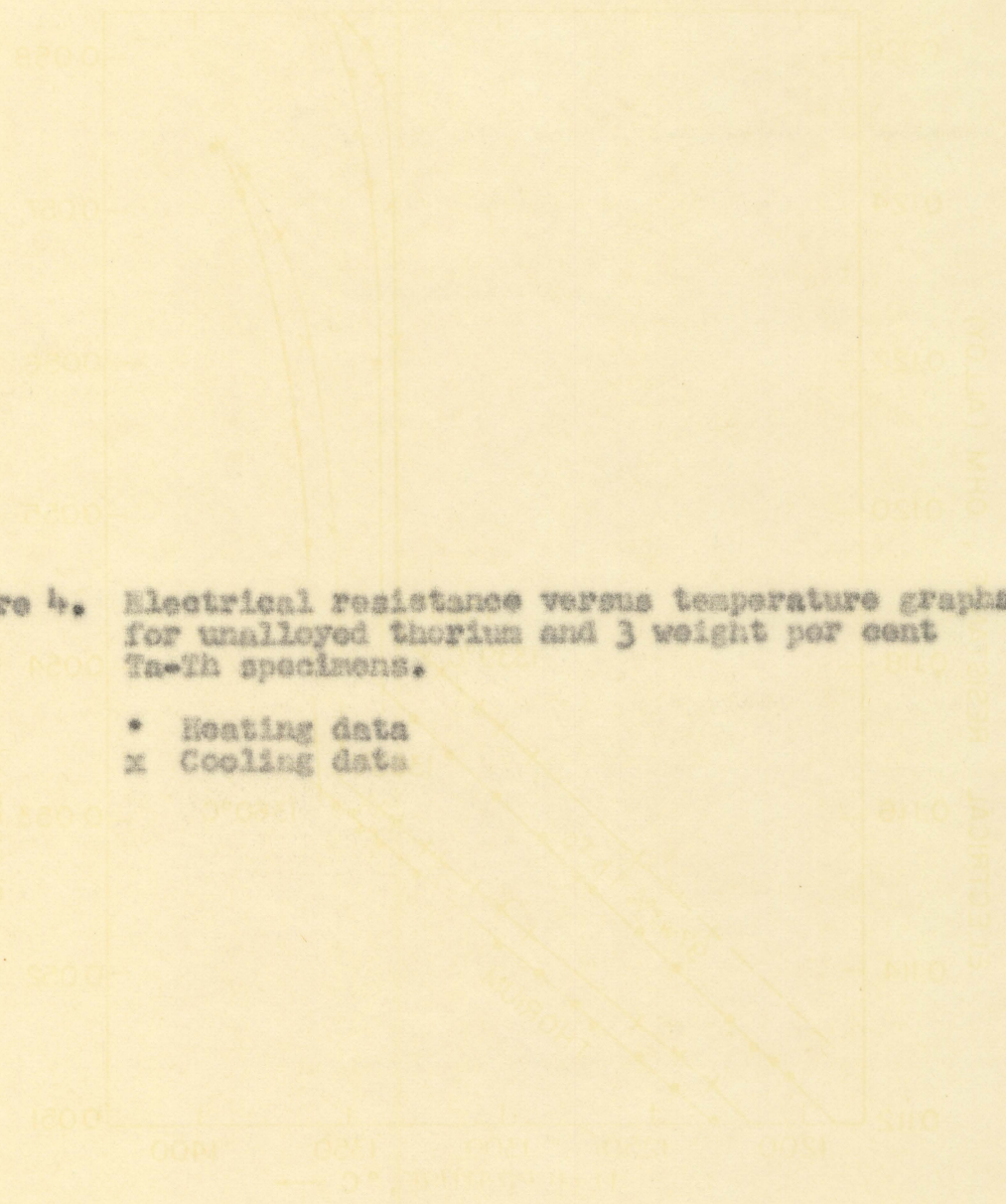
The temperature of the transformation in pure thorium was obtained by averaging the heating curve and cooling curve values from several runs and is $1363 \pm 10^\circ\text{C}$. A temperature of $1338 \pm 5^\circ\text{C}$ was obtained in a similar manner for the alloyed specimens. As indicated by the results obtained

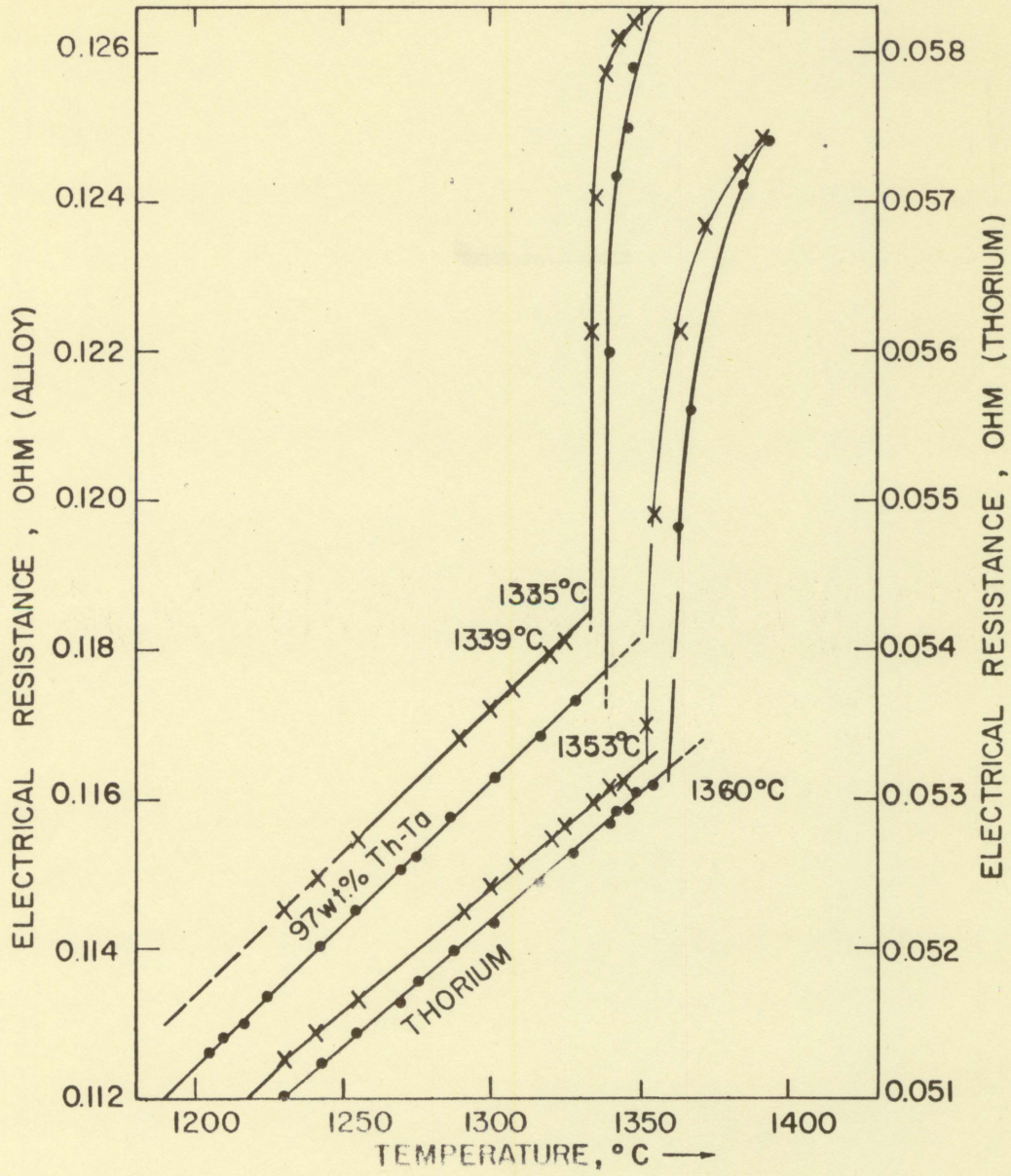
Table 3. Resistance-temperature data

Experiment number	Wt. % Fe-Th	Transformation heating, $^\circ\text{C}$	Temperature cooling, $^\circ\text{C}$
1	thorium 10.0	1365 1335	----- -----
2	thorium 10.0	1367 1338	1362 -----
3	thorium 20.0	1369 1339	1373 1342
4	thorium 10.0	1360 1338	1358 1342
5	thorium	1365	-----
6	thorium 3.2	1368 1339	1353 1335
7	7.5	1338	1333
average for unalloyed thorium		$1363 \pm 10^\circ\text{C}$	
average for alloyed thorium		$1338 \pm 5^\circ\text{C}$	

Figure 4. Electrical resistance versus temperature graphs for unalloyed thorium and 3 weight per cent Ta-Th specimens.

- Heating data
- x Cooling data





from the preliminary resistance-temperature experiments, the addition of tantalum to thorium lowers the transformation temperature and the eutectoidal arrangement is strongly suggested. The $\pm 5^{\circ}\text{C}$ accuracy range, justifiably placed on the transformation temperature value for the alloyed specimens, as compared to the $\pm 10^{\circ}\text{C}$ range for the thorium value suggests that tantalum additions to thorium act as an impurity gettering agent. This phenomenon can best be explained by noting that, as reported by Chiotti (3), tantalum effectively removes carbon from thorium to form insoluble Ta_2C . This fact coupled with the information included in the proposed thorium-carbon phase diagram by Wilhelm (12) helps to explain the accuracy limits of the transformation temperature of thorium observed in these data. From the proposed thorium-carbon diagram it was noted that as little as 100 ppm of carbon in thorium could raise the transformation temperature 15°C and such a study led to the accepted $1360 \pm 10^{\circ}\text{C}$ transformation temperature for pure thorium, which was obtained by extrapolation to zero per cent carbon.

X-ray diffraction data obtained from quenched wire (0.010 inch diameter) specimens using a Debye-Scherrer type camera yielded solubility values which are in agreement with the eutectoidal arrangement suggested by the resistance-temperature results. Precautions were taken in order to minimize the contamination of the freshly prepared specimens

used in the final analysis. A sample set of data and calculations are included as the Appendix so as to facilitate the presentation of the indexing procedure and help to justify the accuracy of the values obtained. Although the thorium lines consist of spots, the various reflections (lines) were distinct and are easily measurable to ± 0.005 centimeters. Thorium oxide patterns were present indicating that the specimens were saturated with oxygen. Three X-ray patterns from different portions of each quenched wire were indexed and the lattice parameters obtained for the individual reflections (a_{hkl}) were averaged. These average a_{hkl} values and their corresponding Nelson-Riley functions (6) were used in the method of least squares, as described by Cullity (4). Accurate lattice parameters, which appear as the y-intercept in the equations of the least squares method are listed in Table 4. The choice of the Nelson-Riley function, as opposed to other possible functions, was made primarily to compensate for the error due to the absorption of the X-rays by the solid specimens. Azaroff and Buerger (1) discuss the merits of the various functions used in the determination of lattice parameters. The solubility data given in Table 4 resulted from the calculations based on the lattice parameter values and it was assumed that Vegard's Law holds for this dilute solution case. The following sample calculation includes correction factors for co-ordination numbers and

for atomic diameter differences due to the packing of the two structures involved. It was also assumed that the solubility data obtained from the analysis of specimens quenched from above the transformation temperature of thorium are representative of this region even though the high temperature crystalline form was not retained in the quenching process.

Calculations yielding Δa_0 as a function of solubility: The lattice parameters of the parent metals as determined experimentally by the method described above are;

$$\begin{array}{ll} \text{Tantalum - b.c.c.} & a_0 = 3.3030 \text{ \AA} \\ \text{Thorium - f.c.c.} & a_0 = 5.0854 \text{ \AA} \end{array}$$

The atomic radius of an atom in a structure whose co-ordination number is 12 contracts about 3 per cent when placed in a structure whose co-ordination is 8.

$$r = \frac{\sqrt{3} a_0}{4} = \frac{\sqrt{3} (3.3030)}{4} = 1.4302 \text{ \AA} \text{ (for b.c.c. Ta)}$$

$$r - 0.03 r = 1.4302 \text{ (contraction)}$$

$$r = 1.4744 \text{ \AA} \text{ (for f.c.c. equivalent Ta)}$$

This size atoms placed in a f.c.c. structure results in an equivalent parameter of

$$2 a_0^2 = (4r)^2 = (4 \times 1.4744)^2 = (5.8976)^2$$

$$a_0 = 4.1703 \text{ \AA} \text{ (f.c.c. equivalent for b.c.c. Ta).}$$

Now: $5.0854 - 4.1703 = 0.9151 \text{ \AA}$ represents 100% solubility.

$\Delta a_0 = 0.0092 \text{ \AA}$ represents 1.0 wt. % Ta solubility in Th.

$\Delta a_0 = 0.0009 \text{ \AA}$ represents 0.1 wt. % Ta solubility
in Th.

The lattice parameter of thorium was determined by averaging values obtained from several specimens quenched from various temperatures. The average value of $5.0874 \pm 0.0004 \text{ \AA}$ resulted from these experiments in which care was taken to minimize specimen contamination. Evans and Raynor (5) listed a number of lattice parameter values reported by various investigators and discussed the necessary precautions that must be taken if accurate values are to be obtained. The evidence of their work pointed toward an a_0 of 5.0843 \AA as the preferred lattice spacing for iodide thorium at room temperature. Their chief concern was the elimination of nitrogen contamination effects on the lattice spacing of thorium and they reported that the iodide thorium contained 0.02% carbon.

X-ray data were obtained for the same area of the diagram using specimens of various sizes and shapes in conjunction with a Debye-Scherrer type camera and a self-focusing back-reflection camera. The specimen contamination precautions taken during the final analyses were not adhered to during the specimen preparation stages of these preliminary experiments. Lattice parameter values ranging from 5.0878 \AA to 5.0886 \AA were obtained for unalloyed thorium, while alloyed specimens yielded values from 5.0866 \AA to 5.0874 \AA . The magnitude of these parameters are comparable to those obtained

from low carbon content samples as reported by Nickelson and Peterson (7) and reveal the need for contamination control as suggested by Evans and Haynor (5). However, it was noted that the alloyed specimens quenched from above the transformation temperature yielded thorium lattice parameters which correspond to slightly greater solubilities of tantalum in thorium than that exhibited by specimens quenched from below the transformation temperature. Consistent conditions of sample preparation, storage of samples when not in use, time and nature of specimen heat treatment, film processing, indexing, etc. were maintained in the final analysis and led to the more reliable results.

As shown in Table 4, the solubility data are based on changes in the fourth place of the lattice parameters. The accuracy of the method is also represented by changes in the fourth place ($\pm 0.0004 \text{ \AA}$) of the lattice parameter values. The fact that the lattice parameter values used in the calculations of the solubilities are relative to the impurity contents of both alloyed and unalloyed wire specimens quenched from both the alpha and beta thorium regions of the diagram influenced the final results of the analysis. On the basis of solubility and resistance-temperature data, both peritectoidal and peritectoidal with a minimum arrangements which could develop as a result of the transformation in thorium can be ruled out. These possibilities were rejected

Table 4. Solubility data obtained by X-ray diffraction methods

Composition wt. % Ta-Th	Temperature of quench $\pm 15^\circ\text{C}$	$a_0, \text{\AA}$	$\Delta a_0, \text{\AA}$	Solubility wt. %
Thorium	1330	5.0853		
	1375	5.0855		
5.1	1330	5.0846		
	1375	5.0838		
10.0	1330	5.0848		
	1375	5.0844		
Alloyed thorium (average)	1330	5.0847	0.0006	Ta in Th 0.06
	1375	5.0841	0.0014	0.15
Tantalum	1350	3.3030		
95.0	1350	3.3032	0.0002	Th in Ta 0.02

because both require that the solubility be greater below the transformation isotherm than above and a peritectoidal arrangement demands an increase in the transformation temperature due to the addition of tantalum. The data fulfill most of the requirements of a eutectoidal arrangement with a maximum in the alpha plus beta two phase region, but the additional information needed to positively establish such an arrangement does not appear practical so far as the net contribution to the investigation is concerned. A simple eutectoidal arrangement which could develop as a result of

the transformation in thorium is allowed on the basis of these data and was postulated as the most probable form of this reaction as shown in Figures 2 and 3.

Solubility Limits

X-ray diffraction and metallographic methods were used to obtain the data on solubilities in the thorium-tantalum system. The solubility information as presented in the preceding section applies to this portion of the report. Briefly, the solvus in the eutectoidal region of the diagram has been placed at less than 0.2 weight per cent Ta-Th and is located at about 0.5 weight per cent Ta-Th at the eutectic temperature. Similar X-ray diffraction techniques were used to obtain solubility data at high temperatures on the tantalum rich side of the diagram. Quenched wire specimens exposed to nickel-filtered copper radiation yielded satisfactory patterns and the least squares method was applied to the a_{hkl} versus Nelson-Riley function data. The lattice parameters and solubility limits that resulted from this study are listed in Table 4. A few tantalum patterns were obtained from wire specimens exposed to zirconium-filtered molybdenum radiation, but the reflections (lines) were generally not resolved well enough to measure accurately. As indicated by the parameter values, there is virtually no solid solubility of thorium in tantalum at 1350°C and less than 0.3 weight per cent Th in Ta at the eutectic temperature was detected by the use of back-

reflection equipment.

Room temperature solubility data were obtained by X-ray diffraction methods using powder specimens. The specimens were filed from the melting point bar samples and then heat treated at 900°C for 16 hours in order to relieve the strains due to the filing operation. The precautions connected with the methods of minimizing the effects of contamination on the lattice parameters as discussed by Evans and Raynor (5) were not taken in these analyses. Also, fourth place accuracy in the parameter values was not obtained. Lattice parameter values of $5.086 \pm 0.001 \text{ \AA}$ for both alloyed and unalloyed thorium powders resulted from this X-ray work. The $\pm 0.001 \text{ \AA}$ accuracy is sufficient to detect 0.1 weight per cent solubility according to the calculations in the preceding section. Since no differences in parameter values could be detected between alloyed and unalloyed specimens, the solubility at room temperature must be less than 0.1 weight per cent on both sides of the diagram.

Both the 1.0 weight per cent Th-Ta and the 1.0 weight per cent Ta-Th as-cast samples and heat treated samples quenched from high temperatures exhibited two phase microstructures.

The extensions of the solidus lines from the eutectic horizontal also appear as dashed lines which begin at the 1565°C solubility limits estimated from the X-ray diffraction data.

Metallographic Results

Eutectic composition

Metallographic methods were used to establish the eutectic composition of the thorium-tantalum system. The as-cast structures of samples with decreasing amounts of tantalum were observed microscopically. The eutectic composition was approached from the tantalum rich side, since the gamma tantalum dendrites that formed on freezing were easily identified. Figures 5, 6, 7 and 8 illustrate the approach to the eutectic composition, which was established at 4 weight per cent Ta-Th by this method. The 6 weight per cent Ta-Th microstructure shown in Figure 7 exhibits a few γ -Ta dendrites and the 2 weight per cent Ta-Th microstructure shown in Figure 9 displays thorium solid solution in a eutectic matrix. Distinct dendrites of thorium solid solution did not form during the freezing process due to the small difference between the liquidus line and the eutectic temperature. A relatively harsh electrolytic etching treatment was required to disclose the thorium solid solution shown in Figure 9, while the γ -Ta dendrites were prominent after the application of a mild etchant for a brief period of time.

No compound formation

Only tantalum solid solution and eutectic were observed in varying proportions in all samples between the eutectic

composition and the solid solution limit. Similarly, only thorium solid solution and eutectic were found on the thorium side of the eutectic. The possibility of compound formation in the thorium-tantalum system was ruled out on the basis of X-ray diffraction patterns from cast and heat treated samples. All of the reflections (lines) of the patterns from all alloys were identified as lines from either alpha thorium solid solution, thorium oxide, or gamma tantalum solid solution structures. The metallographic evidence confirms these X-ray diffraction results.

Solubility evidence

All alloy samples prepared in this investigation exhibited two phase microstructures. The microstructure of an as-cast 1 weight per cent Ta-Th sample is shown in Figure 10. Samples of compositions 1 weight per cent Ta-Th and 99 weight per cent Ta-Th that had been heat treated at 1300°C and 1540°C for several hours displayed two phase microstructures which were not detectably different from those of the as-cast samples. Therefore, solubility limits of less than 1 weight per cent at 1540°C were deduced from this metallographic analysis and are in agreement with the solubility data that resulted from the X-ray diffraction studies. Photomicrographs of 99 weight per cent Ta-Th samples are not included since it was difficult to obtain scratch-free surfaces without drastically over-etching the eutectic

constituent, which causes the composition of the samples to be misrepresented.

Component metals

Figures 11 and 12 are microstructures of as-cast crystalline thorium and tantalum, respectively. The electrolytic etching process used to prepare the surface of the thorium left some black residue which had to be removed by mechanical polishing. Also, staining of the surface usually occurred during the etching treatment. A chemical polishing technique was used in the preparation of the tantalum sample in order to avoid most of the difficulties associated with the abrasives used on the polishing wheels. The abrasive particles unduly scratched and pitted the surface of the relatively soft tantalum. Some residue and stains resulted from the chemical polishing process, which also served as an etchant.

Figure 5. 70 wt. % Ta-Th.
Gamma tantalum
solid solution
dendrites in a
eutectic matrix.

Figure 6. 10 wt. % Ta-Th.
Gamma tantalum
solid solution
dendrites in a
eutectic matrix.

Figure 7. 6 wt. % Ta-Th.
Gamma tantalum
solid solution
dendrites in a
eutectic matrix.

Figure 8. 4 wt. % Ta-Th.
Eutectic.

Above samples etched by swabbing the surfaces for one minute with a 1:5 conc. nitric acid to water solution to which was added 0.25 gm sodium fluosilicate for each 100 ml.

Above samples are in their as-cast condition. X 500.

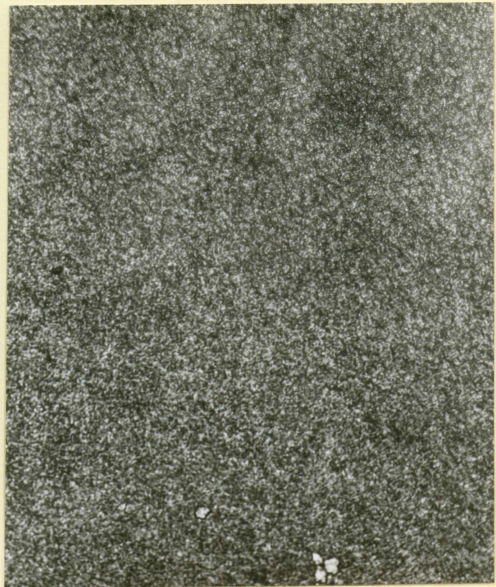
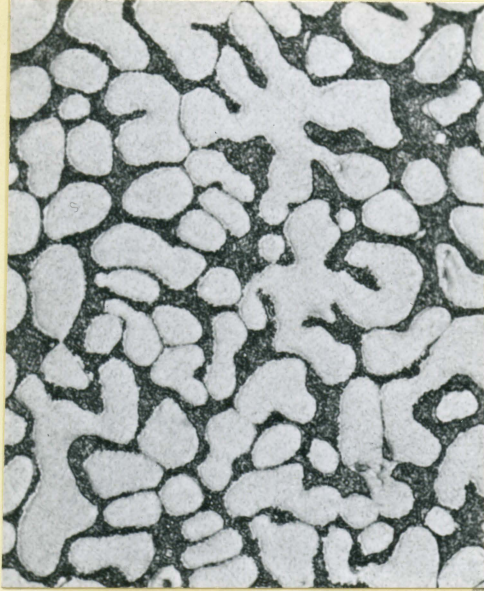


Figure 9. 2 wt. % Ta-Th.
Alpha thorium
solid solution
(light) in a
eutectic matrix.
X 500.

Figure 10. 1 wt. % Ta-Th.
Alpha thorium
solid solution
plus eutectic
(dark). X 500.

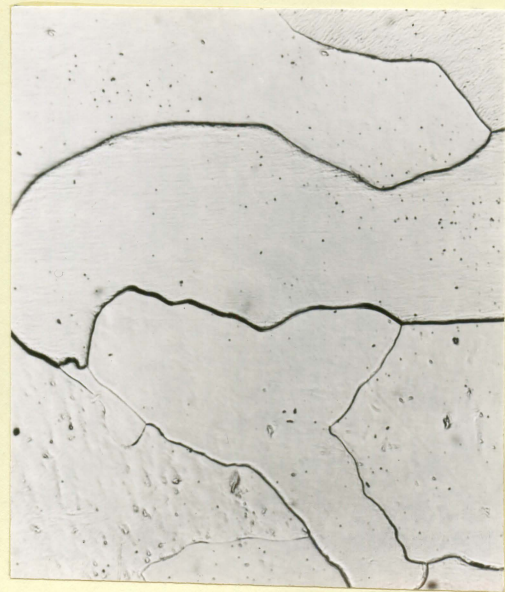
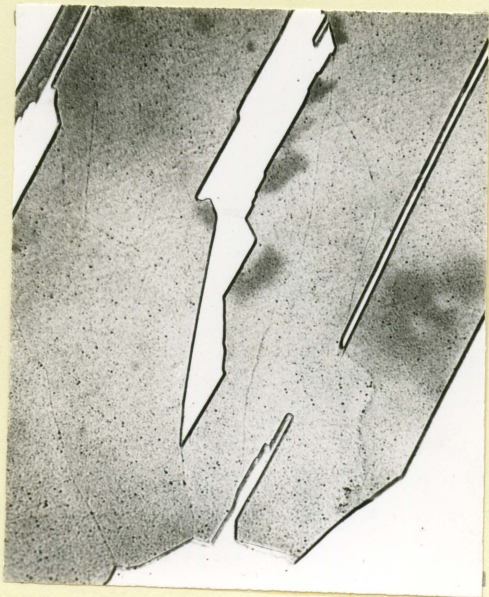
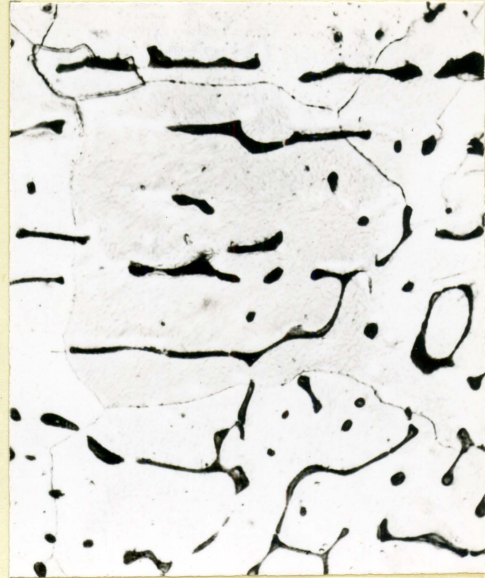
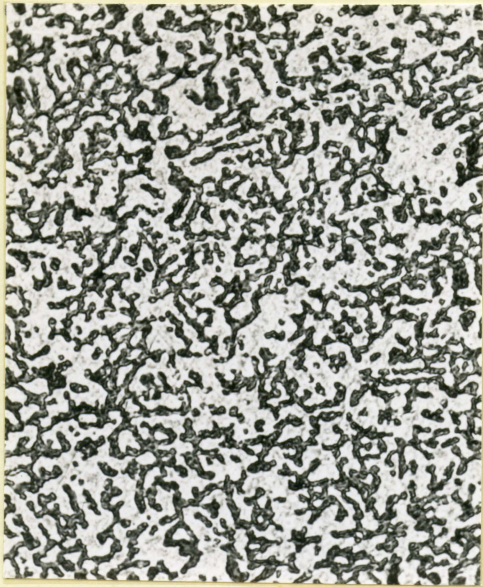
Figure 11. Crystal-bar
thorium. X 150.

Figure 12. Tantalum. X 250.

All samples except Figure 12 etched electrolytically.
Electrolyte 1:1 85% orthophosphoric acid to 90% formic acid.
Exposures of 30 seconds at 35 volts and 0.6 amperes.

Figure 12 sample polished by immersing for 1 minute in a
solution of equal parts of conc. nitric acid, 48% hydrofluoric
acid and lactic acid.

Above samples are in their as-cast condition.



SUMMARY

The thorium-tantalum alloys have been investigated by thermal, microscopic, X-ray diffraction, and electrical resistance methods and a constitutional diagram of the simple eutectic type proposed. The eutectic point occurs at $1565 \pm 10^\circ\text{C}$ and 4 ± 0.5 weight per cent tantalum. No evidence of intermetallic compounds was found and only slight terminal solid solubility was found at either end of the diagram, even at elevated temperatures. The solubility of tantalum in thorium was found to be about 0.4 weight per cent at the eutectic temperature and less than 0.2 weight per cent at the thorium transformation temperature. The eutectoidal arrangement which develops as a result of the transformation in thorium was established on the basis of data from X-ray diffraction and resistance-temperature analyses. The solubility of thorium in tantalum was found to be less than 0.3 weight per cent at the eutectic temperature. The concave liquidus curve on the tantalum rich side of the eutectic composition, if real, suggests that a region of liquid immiscibility nearly exists in the thorium-tantalum system.

ACKNOWLEDGMENTS

The author wishes to acknowledge the advice and counsel of Dr. W. L. Larsen during the progress of this research. Also, acknowledgment is made to Mr. D. E. Williams for his encouragement and assistance in this investigation.

REFERENCES CITED

1. Asaroff, L. V. and Buerger, M. J. The powder method in X-ray crystallography. New York, N.Y. McGraw-Hill Book Co., Inc. 1958.
2. Carlson, A. J., Williams, J. T., Rogers, B. A. and Manthos, E. J. Etching metals by ionic bombardment. U. S. Atomic Energy Commission Report ISC-480. [Iowa State Coll., Ames]. [Office of Technical Services, Washington, D.C.] 1974.
3. Chiotti, P. High temperature crystal structure of thorium. Journal of the Electrochemical Society 101: 567-570. 1954.
4. Cullity, B. D. Elements of X-ray diffraction. Cambridge, Mass. Addison-Wesley Pub. Co. 1956.
5. Evans, D. S. and Raynor, G. V. The lattice spacing of thorium, with reference to contamination. Journal of Nuclear Materials 1: 281-288. 1959.
6. Kempter, C. D. X-ray crystallographic extrapolation functions. U. S. Atomic Energy Commission Report LA-2308. [Los Alamos Scientific Lab., N. Mex.]. [Office of Technical Services, Washington, D.C.] 1959.
7. Mickelson, R. and Peterson, D. Solubility of carbon in thorium. American Society for Metals, Trans. 50: 340-347. 1958.
8. Miller, G. L. Tantalum and niobium. New York, N.Y. Academic Press, Inc. 1959.
9. Rogers, B. A. and Atkins, D. F. Zirconium-columbium diagram. American Institute of Mining and Metallurgical Engineers, Trans. 203: 1034-1041. 1955.
10. Rough, F. A. and Bauer, A. A. Constitutional diagrams of uranium and thorium alloys. Reading, Mass. Addison-Wesley Pub. Co. 1958.
11. Veigel, H. D., Sherwood, E. M. and Campbell, I. E. The preparation of high-purity thorium by the iodide process. U. S. Atomic Energy Commission Report BMI-777. [Batelle Memorial Inst., Columbus, Ohio]. [Office of Technical Services, Washington, D.C.] 1953.

12. Wilhelm, H. A. Thorium. In Finniston, H. M. and Howe, J. P., eds. Metallurgy and fuels. pp. 249-250. New York, N.Y. McGraw-Hill Book Co., Inc. 1956.
13. Williams, D. E. and Pechin, W. H. The tantalum-columbium alloy system. American Society for Metals, Trans. 50: 1081-1089. 1958.
14. Williams, J. T. The vanadium-zirconium alloy system. American Institute of Mining and Metallurgical Engineers, Trans. 200: 345-350. 1955.

APPENDIX

Sample set of data and calculations used to interpret the X-ray diffraction patterns.

Data Sheet 1. Indexing of pattern obtained from an 8 hour exposure of a 5.1 wt. % Ta-Th 10 mil wire specimen quenched from $1330 \pm 15^\circ\text{C}$

Line no.	R, cm.	S, cm.	θ	$\cos^2 \theta$	$\sin^2 \theta$	$n^2+k^2+l^2$	$(a_{hkl})^2$
measured	C-R	S(5.00974)					
0	29.567	average of 12 measurements					
1	26.785						
2	26.355						
3	26.025						
4	25.745						
5	24.970						
6	24.480						
7	24.125						
8	23.525						
9	22.880						
10	22.100						
11	21.960						
12	21.570						
13	21.300	8.267					
14	21.040	8.527					
15	21.005	8.562					
16	19.985	9.582					
17	19.955	9.612					
18	19.190	10.377					
19	19.145	10.422					
20	18.675	10.892					
21	18.635	10.932					
22	17.785	11.782	59.0248	0.264851	0.735119	32	25.82589
23	17.740	11.827	59.2502	0.261418	0.738582		25.83315
24	17.480	12.087	60.5527				
25	17.435	12.132	60.7782	ThO ₂			
26	16.850	12.717	63.7089	0.196189	0.803811	35	25.83319
27	16.790	12.777	64.0095	0.192039	0.807961		25.82872
28	16.515	13.052	65.3871	0.173460	0.826540		36
29	16.455	13.112	65.6877	0.169505	0.830495	25.84591	

Data Sheet 1. (Continued)

Line no.	R, cm. measured	S, cm. C-R	θ S(5.00974)	$\cos^2 \theta$	$\sin^2 \theta$	$h^2+k^2+l^2$	$(a_{hkl})^2$	
30	14.920	14.647	73.3777	0.081831	0.918169	40	25.84644	
31	14.820	14.747	73.8787	0.077102	0.922898		25.84240	
32	13.730	15.837	79.3393					
33	13.570	15.997	80.1468	ThO ₂				
34	12.910	16.657	83.4473	0.013023	0.986977	43	25.84792	
35	12.630	16.932	84.8249	0.008136	0.991864		25.84891	
6	11.602	17.965	average of 16 measurements					

Explanation of calculations involved in Data Sheet 1 by columns:

Column 1 - Line No. - Lines as numbered on the film.

Column 2 - R, cm. - measured by means of the vernier on the film viewer.

Column 3 - S, cm. - front reflection centerline minus individual R's.

Column 4 - theta θ - S times camera constant.

Column 5 - $\cos^2 \theta$ - obtained from tables (6).

Column 6 - $\sin^2 \theta$ - 1 minus $\cos^2 \theta$.

Column 7 - $h^2+k^2+l^2$ - fit of possible f.c.c. reflections to data.

Column 8 - $(a_{hkl})^2$ - from Bragg's Law, $a^2 = \frac{\lambda^2(h^2+k^2+l^2)}{4 \sin^2 \theta}$

$\lambda_{K\alpha 1} = 1.54050 \text{ \AA}$ wavelengths used for the

$\lambda_{K\alpha 2} = 1.54434 \text{ \AA}$ copper radiation data

Data Sheet 2. Least squares method applied to average values of $ahkl$ and Nelson-Riley functions (6) from two patterns (5.1 wt. % Ta-Th)

Nelson-Riley x	x ²	ahkl y	xy
0.011028	0.000122	5.08410	0.056067
0.070165	0.004923	5.08393	0.356714
0.074675	0.005576	5.08402	0.379649
0.166804	0.027824	5.08356	0.847958
0.171273	0.029334	5.08304	0.870588
0.192846	0.037190	5.08240	0.980121
0.197710	0.039089	5.08255	1.004930
0.279490	0.077557	5.08264	1.415464
<u>0.283030</u>	<u>0.080106</u>	<u>5.08192</u>	<u>1.438116</u>
$\Sigma 1.446021$	$\Sigma 0.301721$	$\Sigma 45.74846$	$\Sigma 7.349827$

$$y = a_0 + b_1x$$

$$45.74846 = 9a_0 + 1.446021b_1$$

$$xy = a_1x + b_2x^2$$

$$7.349827 = 1.446021a_1 + 0.301721b_2$$

solving simultaneously;

$$a_0 = 5.08439 = 5.0844 \text{ \AA} = \text{lattice parameter for f.c.c. thorium}$$

in a 5.1 wt. % Ta-Th specimen that had been quenched from

$$1330 \pm 15^\circ\text{C}$$